Atmospheric Environment 72 (2013) 50–59

Contents lists available at SciVerse ScienceDirect

Atmospheric Environment

journal homepage: www.elsevier.com/locate/atmosenv

A proposed physical mechanism for ozone-meteorology correlations using land–atmosphere coupling regimes

Ahmed B. Tawfik [a,b,*], Allison L. Steiner [a]

[a] Department of Atmospheric, Oceanic and Space Sciences, University of Michigan, Space Research Building, 2455 Hayward Street, Ann Arbor, MI 48109-2143, USA
[b] Center for Ocean-Land-Atmosphere Studies, Institute of Global Environment and Society, 4041 Powder Mill Road, Calverton, MD 20705-3106, USA

HIGHLIGHTS

- We propose a physical mechanism producing the ozone-meteorology gradient.
- 17 years of hourly ozone and precursor observations and meteorological data are used.
- Ozone–humidity correlation is an artifact of land–atmosphere coupling regimes.
- Evaporative fraction is a better predictor of ozone for soil water-limited regimes.

ARTICLE INFO

Article history:
Received 30 July 2012
Received in revised form
25 February 2013
Accepted 2 March 2013

Keywords:
Ozone-meteorology correlations
Land–atmosphere coupling
Humidity
Evaporative fraction
Eastern United States
Surface ozone

ABSTRACT

Correlations between surface ozone and meteorological variables exhibit a north-south gradient over the Eastern United States (US), with the ozone–temperature correlation weakening and the ozone–humidity correlation transitioning from positive to negative south of 37°N. Using 17 years of hourly August ozone, nitrogen oxide, and isoprene measurements from the Environmental Protection Agency's Air Quality System and Photochemical Assessment Measurement Stations and hourly meteorological fields from the North American Land Data Assimilation System (Phase 2), we propose that the north-south transition and widely observed ozone–humidity correlation results from a shift in the soil moisture-atmosphere coupling regime. Due to soil water limitations over the Southeast, evapotranspiration and specific humidity increase following precipitation events, and this coincides with reductions in temperature and ozone precursors. Therefore, the negative ozone–humidity correlation in the Southeast is likely a manifestation of several meteorological factors directly influencing ozone production. Surface drying, as defined by the evaporative fraction, provides a better predictor of O_3 than temperature, specific humidity, or radiation for the Southeast due to its ability to retain prior precipitation information and reflect same-day atmospheric conditions relevant to O_3 production. Behavior of surface fluxes and coupling may be particularly relevant for prediction of seasonal and future O_3 air quality, and further investigation into the links between land–atmosphere coupling and O_3 is necessary.

1. Introduction

The Eastern United States (US) is prone to high summer ozone concentrations (O_3) caused by the combination of warm, stagnant meteorological conditions and abundant O_3 precursor species, such as biogenic isoprene (Chameides et al., 1988; Fiore et al., 2005) and anthropogenic nitrogen oxides (Frost et al., 2006). Several modeling (Sillman and Samson, 1995; Dawson et al., 2007; Zeng et al., 2008) and observational (Cox and Chu, 1993; Camalier et al., 2007; Zheng et al., 2007; Bloomer et al., 2009; Blanchard et al., 2010; Davis et al., 2011) studies have found that changes in temperature and humidity are the two primary predictors for O_3 for the Eastern US. This study presents a possible physical mechanism for describing the spatial pattern of temperature- O_3 and humidity- O_3 correlations not yet explained in the literature.

1.1. Surface ozone formation and behavior

Photochemical production of tropospheric O_3 occurs when hydrocarbon species are oxidized by the hydroxyl radical (OH) in the

* Corresponding author. Department of Atmospheric, Oceanic and Space Sciences, University of Michigan, Space Research Building, 2455 Hayward Street, Ann Arbor, MI 48109-2143, USA.
E-mail addresses: abtawfik@umich.edu, abtawfik@cola.iges.org (A.B. Tawfik).

1352-2310/$ – see front matter © 2013 Elsevier Ltd. All rights reserved.
http://dx.doi.org/10.1016/j.atmosenv.2013.03.002

presence of reactive nitrogen oxides (NO_x) and sunlight. This process is accelerated under warmer near-surface conditions; however, the system is highly nonlinear. For example, Steiner et al. (2010) showed that daily 1-h maximum O_3 does not increase with temperatures over 312 K. Further, increased concentrations of atmospheric water vapor can provide a chemical sink for O_3 reducing background concentrations in remote regions through an increased conversion of $O(^1D)$ to OH (Johnson et al., 1999). However, urban studies indicate that loss of O_3 through this pathway is weak (Dawson et al., 2007), and in high NO_x environments increased water vapor can lead to additional OH formation (Steiner et al., 2006) and increased ozone production (Kleinman et al., 2005).

Using statistical methods, Camalier et al. (2007) demonstrated that primary O_3-predictor variables have a clear north-south transition, where high latitude O_3 (>38°N) is strongly positively correlated to daily maximum temperature and lower latitude O_3 (<36°N) strongly negatively correlated to relative humidity. Davis et al. (2011) found that a widely used air quality model does not accurately capture the location of the north-south transition and underestimates the sensitivity of daily maximum 8-h O_3 to temperature and relative humidity. Rasmussen et al. (2012) used a coupled chemistry-climate model to show that the temperature-ozone relationship is overestimated north of 37°N and underestimated farther south. Both studies (Davis et al., 2011; Rasmussen et al., 2012) note that this north-south behavior suggests a latitudinal shift in the regime controlling O_3 and may reflect inherent weaknesses in model meteorology or physics.

1.2. Land–atmosphere–chemistry interactions

Although there is agreement that temperature is a strong controller of O_3 in the Northeast US, warmer temperatures often coincide with other meteorological conditions favorable to O_3 production (Vukovich, 1995), such as stagnation events and reduced cloud cover. Cloud cover changes have been suggested as a possible cause of the negative O_3-humidity correlation in the Southeastern US (Camalier et al., 2007; Davis et al., 2011), yet modeling studies have found that radiation perturbations from cloud cover produce minimal changes in surface O_3 (Sillman and Samson, 1995; Dawson et al., 2007). Another modeling study found that drier soil moisture initialization increased sensible heat flux and warmed temperatures, promoting higher O_3 throughout the boundary layer (Jacobson, 1999), pointing to a possible connection between soil moisture and O_3.

From the climate perspective, soil moisture is known to strongly influence sub-seasonal temperature and precipitation (Findell and Eltahir, 1997; Fennessy and Shukla, 1999; Pal and Eltahir, 2001; Fischer et al., 2007; Wu et al., 2007; Koster et al., 2010; Guo et al., 2011) because soil can retain information of prior precipitation events long after an event has passed. In some regions, this leads to changes in surface flux partitioning where drier (wetter) soils reduce (promote) subsequent precipitation and increase (decrease) temperatures. Near-surface water vapor also decreases over drier soils where soil water controls evapotranspiration (Betts, 2004, 2009; Santanello et al., 2011). This interaction between the soil and atmosphere is known as "land–atmosphere coupling" and can be categorized by two regimes: 1) evapotranspiration is limited by soil water availability, referred to as soil moisture-limited, and 2) evapotranspiration is limited by evaporative energy, referred to as energy-limited (Seneviratne et al., 2010). For soil moisture-limited regimes, the land surface impacts the atmosphere more readily leading to negative (positive) correlations between near-surface temperature (humidity) and evapotranspiration. When evapotranspiration is energy-limited, atmospheric conditions exert control over evapotranspiration with weak feedback from soil moisture.

Here we propose a mechanism that approaches the north-south shift in ozone-meteorology correlations from the perspective of land–atmosphere interactions. By using the land–atmosphere coupling framework, the degree of coupling between surface and atmospheric variables can first be examined and then evaluated within the context of ozone production. This provides the necessary physical basis for describing ozone-meteorology relationships within the coupled climate system. We present evidence that the latitudinal change in ozone–specific humidity correlations likely arise from evapotranspiration-limiting regimes. In this regard, near-surface specific humidity (hereinafter, "humidity") acts as a passive surrogate in ozone formation rather than a direct causal variable. Evidence for this mechanism is explored using observational and reanalysis data over the Eastern US.

2. Data and methods

2.1. Observational chemical concentrations

Hourly O_3, NO_y, NO_x, and isoprene concentration data for August from 1994 to 2010 are obtained from the Environmental Protection Agency's Air Quality System (EPA-AQS) Photochemical Assessment Monitoring Stations.[1] Analysis is confined to stations within the Eastern US (25–50°N and 98–68°W). In this region, there are a total of 1221, 71, 376, and 223 stations measuring O_3, NO_y, NO_x, and isoprene, respectively, with at least 650, 16, 126, and 30 active stations for any given year from 1994 through 2010. Ozone data are filtered to include stations and years with at least half a month of hourly measurements. Precursor species (NO_y, NO_x, and isoprene) data are not filtered due to limited data availability and to provide the maximum number of measurements for evaluation. The measurement method used for NO_x in the EPA-AQS network has been shown to erroneously include peroxy acetyl nitrate (PAN), organic nitrates, and nitric acid (HNO_3) (Fehsenfeld et al., 1987; Dunlea et al., 2007). Therefore, NO_x measurements are treated as containing a subset of nitrogen oxide species that may be more effectively wet removed than NO_x (=NO_2 + NO). August is selected in this study due to peak summer temperatures and the potential for O_3 exceedances.

2.2. North American land data assimilation system

A suite of atmospheric and land surface data from Phase 2 of the North American Land Data Assimilation System (NLDAS2) is used for the climate data analysis. NLDAS2 provides hourly 2-m temperature, incident solar radiation (R), 2-m humidity, and precipitation at 1/8° by 1/8° degree grid spacing from 1994 to 2010 (Mitchell et al., 2004). With the exception of precipitation, NLDAS2 atmospheric forcing fields are elevation-adjusted quantities derived from the North American Regional Reanalysis (NARR; 32 km by 32 km) (Mesinger et al., 2006) and are temporally interpolated from 3-hourly to hourly, and spatially interpolated to the higher eighth-degree grid spacing required by NLDAS2 (Cosgrove et al., 2003). Incident radiation is bias-corrected using 5 years of hourly GOES-8 satellite data (Pinker et al., 2003). Precipitation is derived from PRISM topographically adjusted daily Climate Prediction Center (CPC) precipitation gauge data (Daly et al., 1994; Xie and Arkin, 1997) and is temporally decomposed into hourly

[1] US EPA, 2011 Air Quality System Data Mart: US Environmental Protection Agency http://www.epa.gov/ttn/airs/aqsdatamart.

data using Stage II 4 km by 4 km hourly Doppler radar output or the CPC Hourly Precipitation Dataset (HPD) (Higgins et al., 1996). Surface variables (soil moisture, net surface radiation (R_n), and surface fluxes (sensible, H, and latent flux, λE)) are acquired from NLDAS2-MOSAIC land surface model (Koster and Suarez, 1992, 1994). NLDAS2-MOSAIC is forced by NLDAS2 atmospheric fields, including surface pressure and 10-m wind components in addition to the variables described above. To avoid any single grid cell bias, NLDAS2 data are averaged over a 1/4° by 1/4° region around each EPA-AQS station.

2.3. Soil moisture-temperature coupling parameter

Several observed (Koster et al., 2009; Dirmeyer, 2011; Miralles et al., 2012) and model-based (Koster et al., 2006; Seneviratne et al., 2006) metrics have been developed to quantify land–atmosphere coupling, and these methods generally identify coupling in the same geographic areas (Seneviratne et al., 2010; Miralles et al., 2012). To identify factors limiting surface evapotranspiration, we employ a soil moisture-temperature coupling diagnostic ($\rho(E,T)$) defined as the Pearson correlation between evapotranspiration (E) and temperature (T) (Seneviratne et al., 2006). Negative values of $\rho(E,T)$ are referred to as soil moisture-limited or "coupled" while positive values are energy-limited or "uncoupled". We calculate a modified monthly version of $\rho(E,T)$ using midday average (12pm–4pm) E and T for each August (e.g. the correlation between 31 days of E and T for each year).

3. Results

3.1. Spatial patterns of ozone concentrations and correlations

Average August midday (12–4pm) O_3 over the Eastern US is between 45 and 65 ppb with the highest concentrations occurring along the Eastern Seaboard, the Ohio River Valley, and Tennessee River Valley (Fig. 1a). Fig. 1b shows the correlation between O_3 and temperature ($\rho(T,O_3)$) for August at each EPA-AQS station with at least 10 years of data. Consistent with prior studies (Camalier et al., 2007; Davis et al., 2011; Rasmussen et al., 2012), temperature is most strongly correlated to O_3 north of 38°N ($\rho(T,O_3) > 0.7$) and weakens south of 36°N ($\rho(T,O_3) < 0.5$). The correlations between humidity and ozone ($\rho(q,O_3)$; Fig. 1c) show similar north-south decreases as $\rho(T,O_3)$, but with a transition from positive to negative correlation coefficients south of 37°N.

3.2. Meteorological and climate controls on ozone

Zonally averaged anomalies can be used to understand environmental controls on O_3 interannual variability (Fig. 2), where anomalous conditions are defined as deviations from the 1994–2010 mean August conditions at EPA-AQS stations. In 1999, O_3 anomalies reach 12 ppb from 30 to 36°N (Fig. 2a), and 4–7 ppb higher, during the historic 2007 drought in the Southeast (Luo and Wood, 2007). The lowest O_3 anomalies occurred in 2009 from 32 to 38°N and were more than 10 ppb below the 17-year average during a year with anomalously wet soil moisture conditions (Fig. 2d).

During the years with the greatest positive anomalies of O_3 (1999, 2000, and 2007), R and temperature anomalies are also higher than average (Fig. 2b and c, respectively). For 1999 and 2000, R was about 40 W m^{-2} greater than the 17-year mean and 20–50 W m^{-2} greater for 2007 over the Southeastern US, suggesting a reduction in cloud cover. Warm temperature anomalies are concurrent with R anomalies, with 2007 as the warmest year in the Southeast (>3 K), and 1999 and 2000 having weaker but non-negligible positive anomalies (0.5–3 K). Temperature anomalies also correspond to drier than average soil moisture conditions (Fig. 2d), with 2000 and 2007 as the driest years. Soil moisture spatial anomalies follow the same pattern as temperature anomalies in the Southeast consistent with the land–atmosphere coupling framework presented in Section 1.2 highlighting the potential for land–atmosphere interactions to modulate O_3.

3.3. Land–atmosphere coupling and ozone

The soil moisture-temperature coupling parameter ($\rho(E,T)$; Section 2.3) calculated from NLDAS2 data (Fig. 3) shows a similar spatial behavior as $\rho(q,O_3)$ (Fig. 1c). Specifically, stations where soil moisture perturbations exert greater control on near-surface temperatures (e.g. $\rho(E,T) < 0$) correspond to stations with a weaker $\rho(T,O_3)$ and negative $\rho(q,O_3)$ (Fig. 1b and c). This suggests that the ozone-meteorology correlations may be influenced by land–atmosphere interactions over the Southeastern US.

To understand the relationships between predictor climate variables (T, q, R) and O_3 we examine the zonally averaged interannual changes in $\rho(E,T)$ (Fig. 4a). For stations south of 36°N, evapotranspiration is soil moisture limited ($\rho(E,T) < 0$) for all years except 2009 (Fig. 4a). North of 40°N, evapotranspiration tends to be energy-limited ($\rho(E,T) > 0$). In the Mid-Atlantic region (36–39°N)

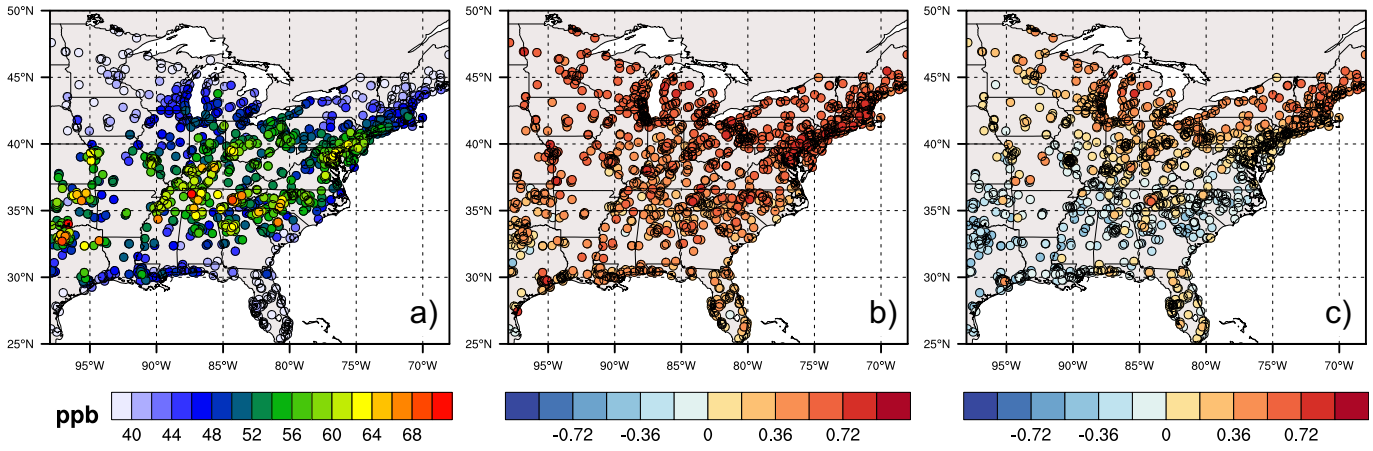

Fig. 1. a) August observed midday (12–4pm) average surface ozone concentrations (ppb), and Pearson's correlation coefficient of ozone versus Phase 2 NLDAS reanalysis 2-m b) temperature and c) humidity from 1994 to 2010 at EPA-AQS stations.

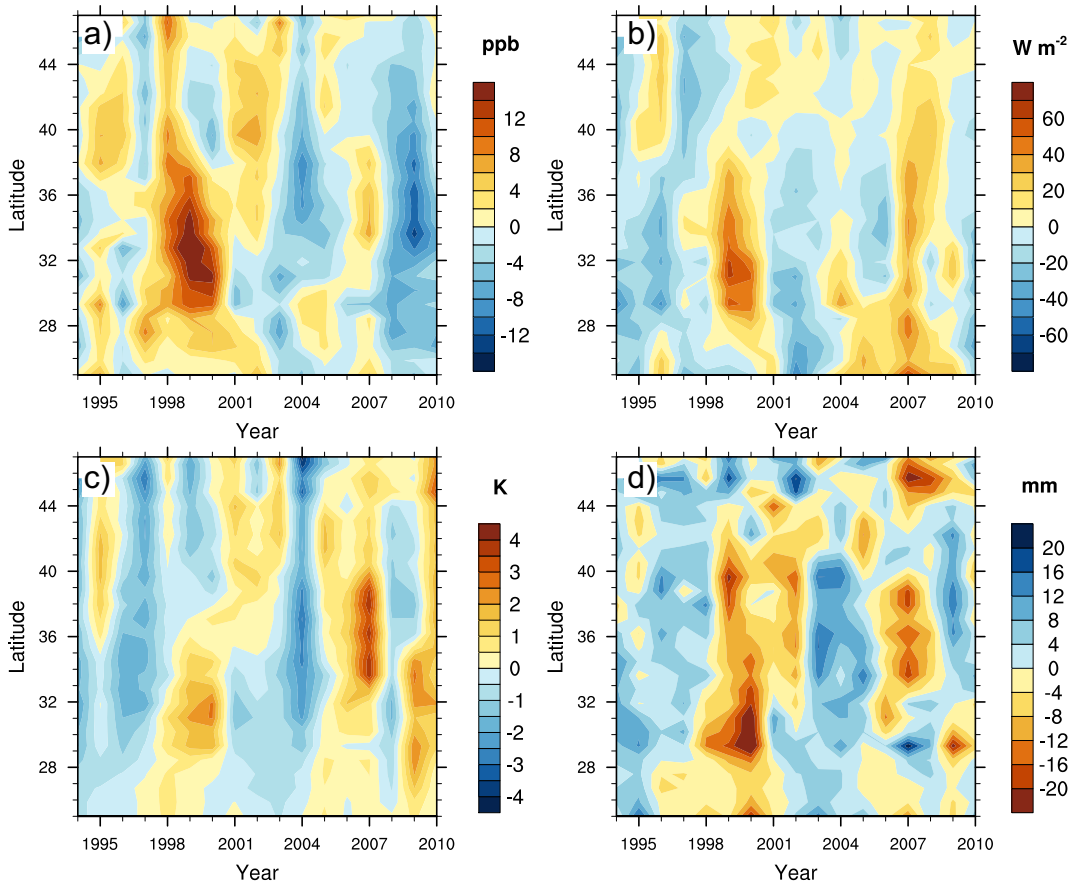

Fig. 2. Zonally averaged anomalies for observed average midday a) surface ozone concentrations (ppb), b) NLDAS2 reanalysis incident solar radiation (W m^{-2}), c) NLDAS2 reanalysis 2-m temperatures (K), and d) NLDAS2-MOSAIC reanalysis soil moisture from 0 to 40 cm (mm) for August from 1994 to 2010 at EPA-AQS stations.

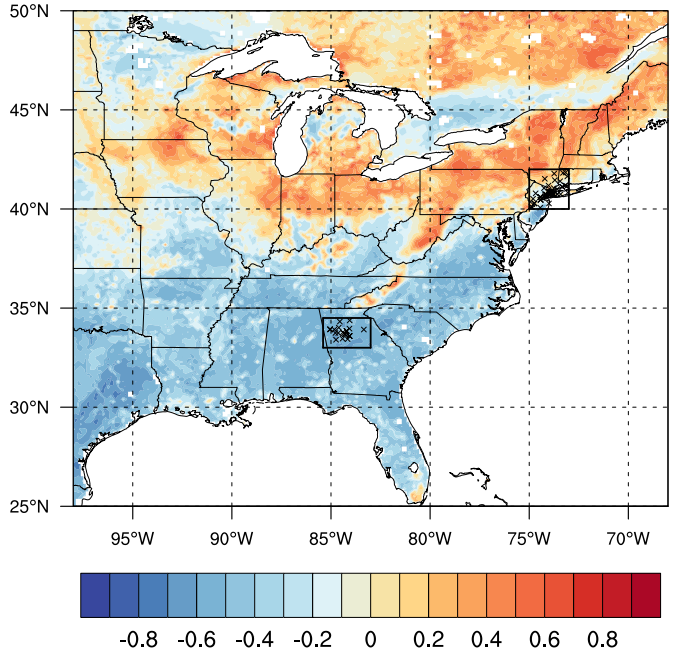

Fig. 3. Pearson's correlation between NLDAS2 reanalysis evapotranspiration (E) and 2-m temperature (T). Markers indicate particular EPA-AQS-PAMS stations for the Northeast (NE) and Atlanta Metropolitan Area (ATL) averaging regions: 46 (NE) and 16 (ATL) ozone stations, 20 (NE) and 5 (ATL) NO_x stations, zero (NE) and 3 (ATL) NO_y stations, and 11 (NE) and 4 (ATL) isoprene stations.

the limiting factor varies interannually, indicative of a regime shift as suggested by Davis et al. (2011) and Rasmussen et al. (2012).

Zonally averaged correlations between midday O_3 and environmental variables exhibit north-south features similar to the coupling parameter (Fig. 4b). Consistent with station data in Fig. 1, temperature is positively correlated with O_3 throughout the Eastern US with stronger correlations at higher latitudes (Fig. 4b; $\rho(O_3,T) = 0.1–0.6$). In contrast, $\rho(O_3,q)$ exhibits a latitudinal gradient with a transition from negative values in the South (<36°N) to positive values in the North (>39°N). This transition occurs in the same Mid-Atlantic region (36–39°N) coinciding with the transition from soil water-limited to energy-limited regimes (Fig. 3). The transition zone corresponds to the region where mid-latitude synoptic systems become less prominent and convective events dominate (Li et al., 2005; Leibensperger et al., 2008; Fang et al., 2009). R is positively correlated with midday O_3 at each zonal band with the strongest correlations from 33 to 40°N ($\rho(O_3,R) = 0.3–0.4$).

The evaporative fraction ($\lambda E/R_N$) defines the portion of net surface radiation (R_N) partitioned to evapotranspiration and can describe the degree of surface drying. $\lambda E/R_N$ is negatively correlated with O_3 over the Eastern US and the absolute value of $\rho(O_3, \lambda E/R_N)$ is greater than those of $\rho(O_3,T)$ or $\rho(O_3,q)$ ($\rho(O_3, \lambda E/R_N) < -0.6$) south of 39°N (Fig. 4b). Given the strong correlation between $\lambda E/R_N$ and O_3, $\lambda E/R_N$ may prove to be a better O_3 predictor than other more commonly used variables for the Southeastern US. The correlation with midday O_3 weakens to the north (>39°N) where evapotranspiration is no longer soil moisture limited. The physical mechanism underlying the strength of evaporative fraction as a

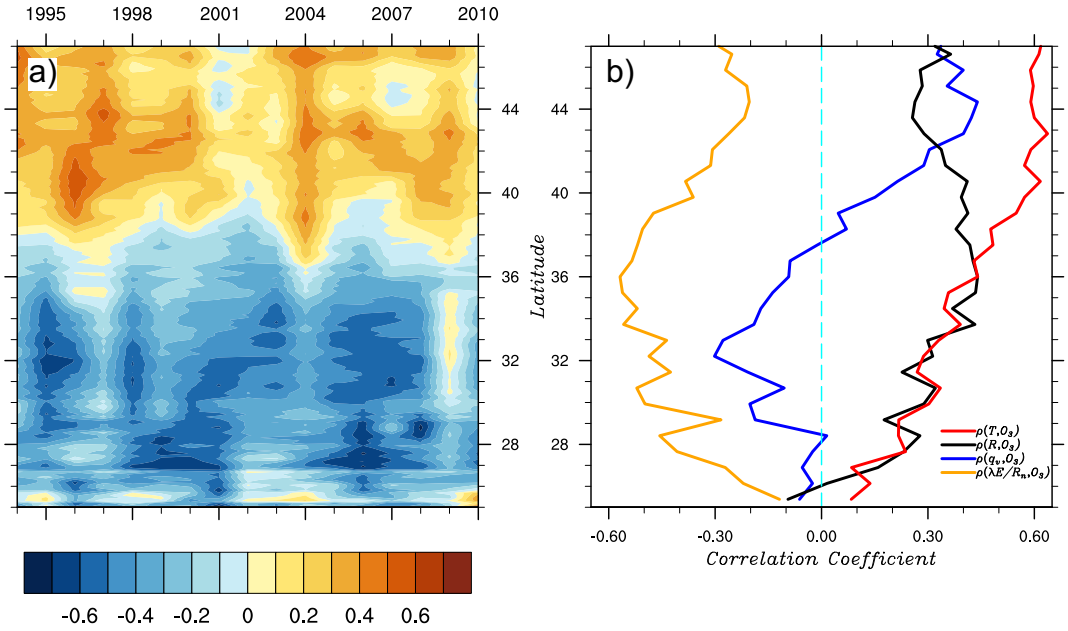

Fig. 4. August zonally averaged (a) interannual variations in soil moisture–temperature coupling strength ($\rho(E,T)$; Section 2.2) derived from NLDAS2 reanalysis and (b) zonally averaged correlation coefficient of observed midday average ozone against NLDAS2 reanalysis derived (red) 2-m temperature, (black) incident radiation, (blue) 2-m humidity, and (orange) evaporative fraction. (For interpretation of the references to color in this figure legend, the reader is referred to the web version of this article.)

predictor and the latitudinal behavior of correlations is described in Section 4.

3.4. Antecedent meteorological behavior

To further evaluate our proposed physical mechanism, we examine the average antecedent temporal evolution of meteorology (Fig. 5) and chemical species (Fig. 6) prior to low (<40 ppb) and high (>70 ppb) midday O_3 events. Two regions are examined, the Atlanta Metropolitan area (33–34.5°N and 83–85.4°W; ATL; soil-moisture limited) and a Northeast region (40–42°N and 73–75°W; NE; energy-limited), to represent typical urban O_3 non-attainment environments with long time series of chemical concentrations corresponding to different land–atmosphere coupling regimes. An average of all August high (142 for ATL; 78 for NE) and low (88 for ATL; 145 for NE) O_3 days from 1994 to 2010 are presented in Figs. 5 and 6. Other geographic regions were examined and returned similar results (see Supplementary material).

Average meteorological conditions (temperature, precipitation, humidity, wind speed) leading up to high and low O_3 events are presented in Fig. 5. Comparing ATL and NE, there is a noticeable decrease (increase) in 2-m temperatures over the course of the 96 h prior to low (high) O_3 events with a greater temperature change for NE (Fig. 5a). Both regions also record warmer temperatures prior to high O_3 events. Accumulated precipitation totals for the 96 h prior demonstrate an even greater response between high and low O_3 days for both regions (Fig. 5b). Precipitation totals are on average 19 mm prior to low O_3 events and less than 6 mm for high O_3 days. The difference in antecedent precipitation between high and low O_3 events weakens beyond 60 h prior and converges at 4 mm, demonstrating that the influence of antecedent precipitation on midday O_3 is approximately two days.

In the NE, humidity gradually increases leading up to high O_3 days (>70 ppb) from an average of 13–14.5 g kg^{-1}, with a sharper rise 36 h prior to the O_3 maxima (Fig. 5c). This sharp increase coincides with warmer temperatures and less precipitation relative to low O_3 days and may be indicative of a change in air mass following frontal passage. For ATL, high O_3 days correspond to lower midday humidity (~14.2 g kg^{-1}; Fig. 5c) whereas humidity increases slightly during the hours prior to low O_3 conditions. Antecedent midday (12–4pm) average evaporative fraction ($\lambda E/R_N$) for ATL exhibits a 15% decrease in energy partitioning toward evapotranspiration under high O_3 and ~20% increase under low O_3 (Fig. 5d). Overall, 90% of high (low) O_3 days have midday average $\lambda E/R_N$ less (greater) than 0.5 for ATL. For NE, only 60% of high O_3 days have $\lambda E/R_N$ less than 0.5 and weaker evaporative fraction changes of 2% and 10% prior to high and low O_3 conditions, respectively. This weaker response of evaporative fraction for the NE relative to ATL under comparable antecedent precipitation behavior further suggests a difference in land–atmosphere coupling regimes. Specifically, the evaporative fraction is less responsive to precipitation in the NE region as expected for energy-limited regimes.

Stagnant air masses have been shown to promote pollutant accumulation (Vukovich, 1995) and are negatively correlated with the number of mid-latitude cyclone passages (Leibensperger et al., 2008). Using NLDAS2 10-m surface wind speed as an indicator of stagnation (Fig. 5e), winds are generally lighter approaching high O_3 events indicating more stagnant conditions in both regions. For ATL, winds are ~2 m s^{-1} weaker for high O_3 events with a weaker diurnal cycle (Fig. 5e), similar to results discussed in Blanchard et al. (2010). The NE exhibits weaker winds (~2 m s^{-1}) only during the nighttime hours prior to high O_3 events, with little change during the day (0–0.6 m s^{-1}). An inland energy-limited region was also examined (see Supplementary material) and showed similar wind speed behavior as the NE region with little contrast in wind speed during the day between high and low O_3 events, but calmer winds at night for high O_3 events. Therefore, the diurnal wind behavior seen in the NE is likely not a result of its proximity to the Atlantic Ocean and a land–sea breeze.

3.5. Antecedent precursor behavior

The behavior of O_3 and its precursors (NO_x, NO_y, and isoprene) are examined to identify the impacts of atmospheric and surface

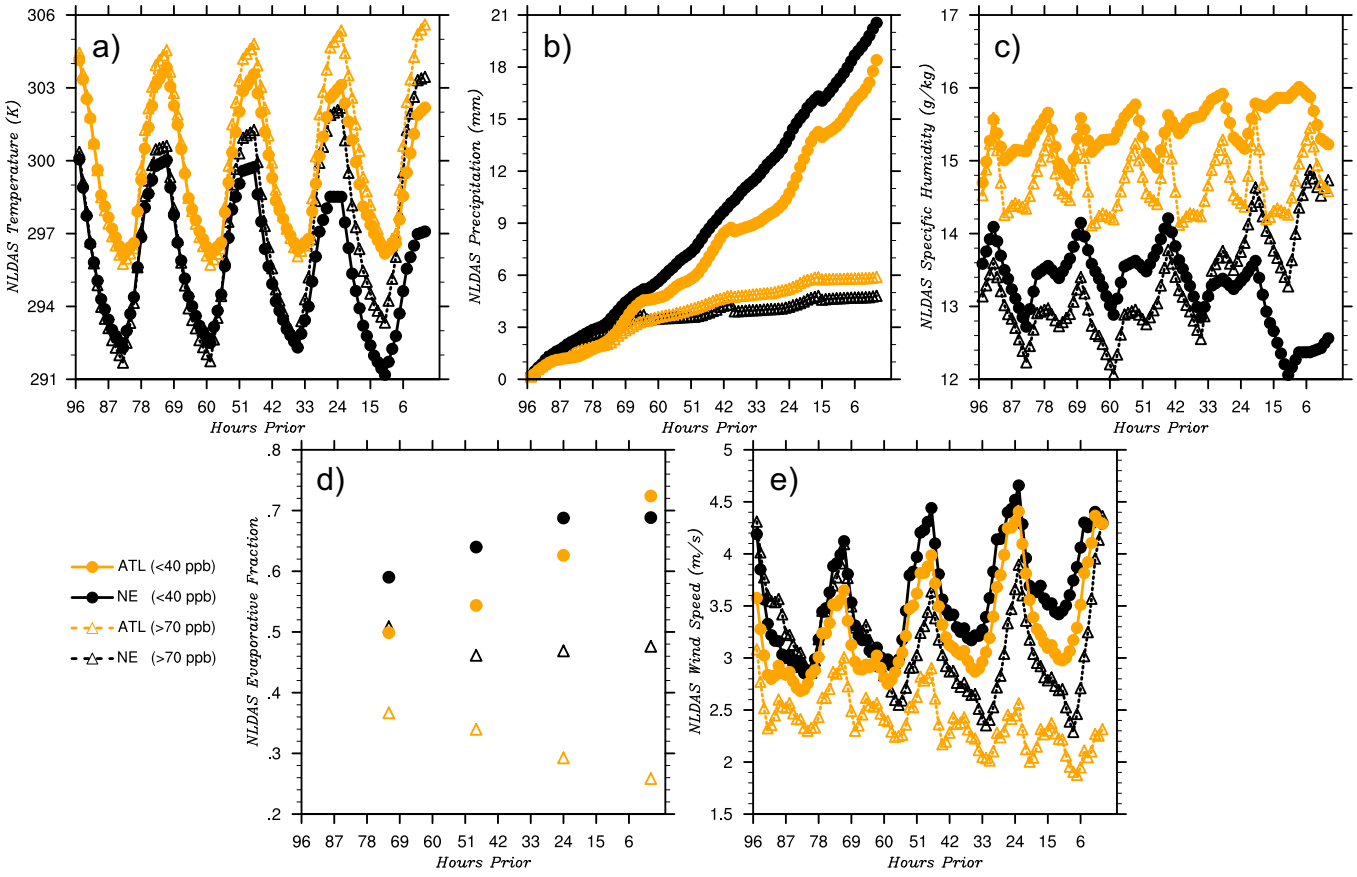

Fig. 5. Antecedent August a) 2-m temperature (K), b) accumulated precipitation (mm), c) 2-m humidity (g kg^{-1}), d) evaporative fraction, and e) 10-m wind speed (m s^{-1}) from NLDAS2 reanalysis for the hours approaching high (>70 ppb; dashed) and low (<40 ppb; solid) midday ozone concentrations averaged over EPA-AQS-PAMS sites for NE (black) and ATL (orange) from 1994 to 2010. NE and ATL regions defined in Fig. 3. (For interpretation of the references to color in this figure legend, the reader is referred to the web version of this article.)

conditions on air quality (Fig. 6). For ATL, NO_x is on average below 10 ppb prior to low O_3 events and reaches 60 ppb approaching high O_3 events (Fig. 6b). The difference in antecedent NO_x concentrations between high and low O_3 events is less pronounced for the NE with prior morning and nighttime (6–20 h prior) NO_x concentrations of 20–32 ppb for low O_3 events and 40–64 ppb for high O_3events. Generally, the NE has higher midday NO_x (~20 ppb) than ATL (~4 ppb; Fig. 6b).

Elevated isoprene can increase photochemical O_3 production under sufficiently high NO_x (Chameides et al., 1988; Fiore et al., 2005). Isoprene concentrations range from <1 ppb on average at night to almost 4 ppb during the day for ATL (Fig. 6c), reflecting the strong biogenic isoprene source region in the Southeastern US (Guenther et al., 2006). The NE has lower isoprene with average midday values less than 1.5 ppb. Comparing the hours approaching high and low O_3 for both regions, higher isoprene concentrations correspond to high O_3 days and are likely driven by the warmer temperatures (1–4 K for ATL and 2–6 K for NE; Fig. 5a) resulting in higher biogenic isoprene emissions (Guenther et al., 1994; Petron et al., 2001).

Although NO_y measurements are only available for the ATL region, antecedent NO_z (NO_y–NO_x) identifies the behavior of the primary chemical sink of NO_x and the importance of wet removal. Antecedent NO_z is 10 ppb higher the night before high O_3 days, with little difference in high and low events prior to 20 h (Fig. 6d). The higher NO_z concentrations observed prior to high O_3 events correspond to dry (Fig. 5d) and stagnant conditions (Fig. 5e) with less wet removal (Fig. 5b).

4. Discussion

Here we describe a mechanism controlling ozone-meteorology correlations under two soil moisture–atmosphere coupling regimes: 1) energy-limited evapotranspiration and 2) soil moisture-limited evapotranspiration. Environmental and chemical conditions leading up to high O_3 events for energy-limited regimes (e.g., NE) are characterized by: little precipitation, weak changes in energy partitioning, warmer temperatures, higher humidity, more stagnant nighttime conditions, higher nighttime NO_x concentrations, and slightly higher isoprene concentrations relative to low O_3 events (Figs. 5 and 6). The hours prior to high O_3 events for soil moisture-limited regimes (e.g., ATL) are characterized by: little precipitation, less energy partitioning toward evapotranspiration, warmer temperatures, lower humidity, more stagnant conditions, higher nighttime NO_x and NO_z concentrations, and slightly higher isoprene relative to low O_3 events (Figs. 5 and 6). The two regimes differ only in the behavior of evaporative fraction and humidity suggesting that the commonly observed ozone–humidity correlation over the Southeastern US may be a manifestation of soil moisture–atmosphere coupling regimes. This proposed physical mechanism is described below and summarized in Fig. 7.

Precipitation events in both coupling regimes directly modify the chemical and meteorological environment. From the chemical perspective, greater precipitation effectively removes NO_y species (Figs. 5b, 6b and d) through ventilation (Pickering et al., 1988; Vukovich, 1995), outflow (Merrill and Moody, 1996; Li et al., 2005; Leibensperger et al., 2008; Fang et al., 2009), and wet removal

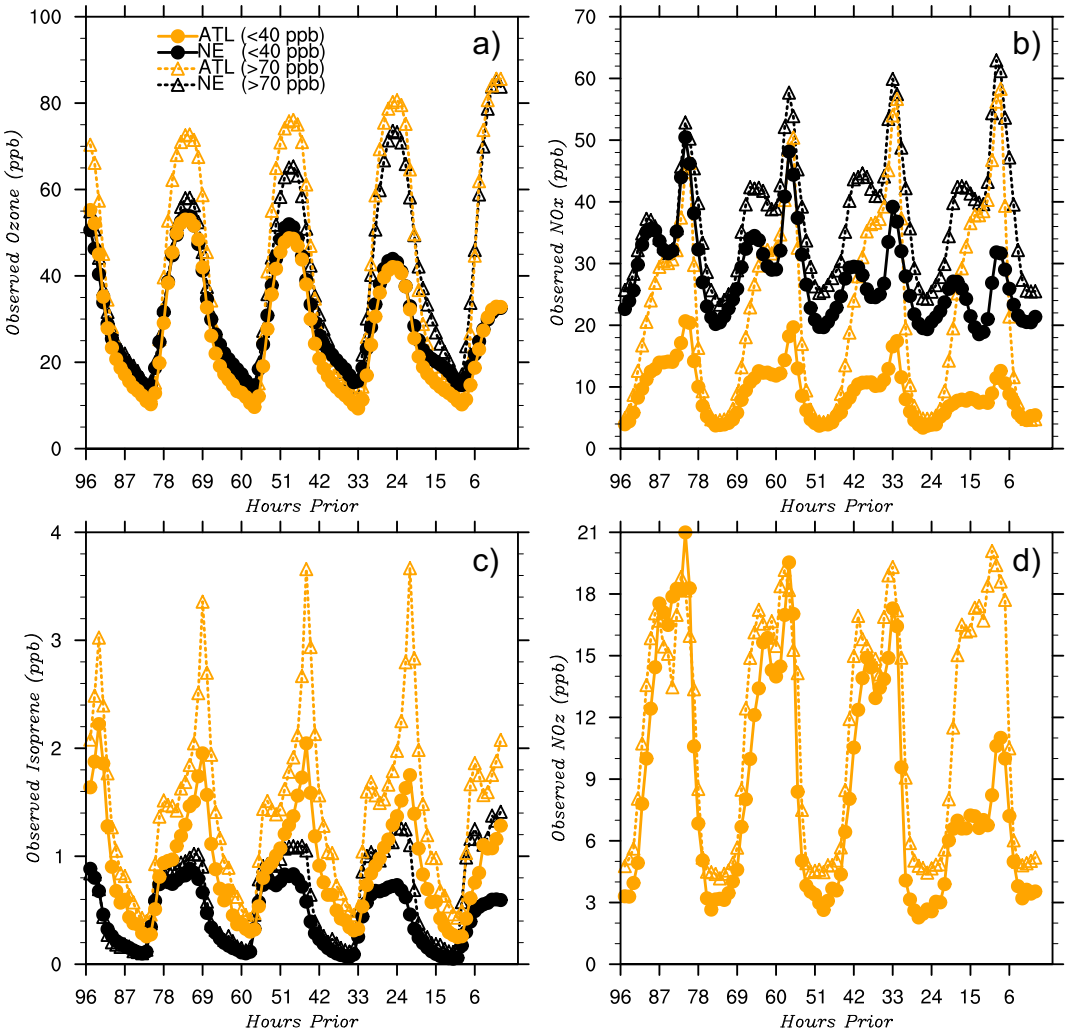

Fig. 6. As in Fig. 5, but for observed antecedent a) ozone, b) NO_x, c) isoprene, and d) NO_z (NO_y–NO_x) concentrations (ppb) for hours approaching high (>70 ppb; dashed) and low (<40 ppb; solid) midday ozone concentrations for a region in the Northeast (NE; black) and region around the Atlanta Metropolitan area (ATL; orange). (For interpretation of the references to color in this figure legend, the reader is referred to the web version of this article.)

(Sickles and Shadwick, 2007) reducing ozone concentrations the following day (Figs. 6a and 7). This ozone precursor removal occurs in both coupling regimes but the nature of the precipitation event varies. In the case of energy-limited regimes (north of 37°N), precipitation events are generally driven by synoptic events, such as frontal passages or mid-latitude cyclones (Whelpdale et al., 1984; Merrill and Moody, 1996; Leibensperger et al., 2008) supplying a cooler and less humid air mass following passage. This is

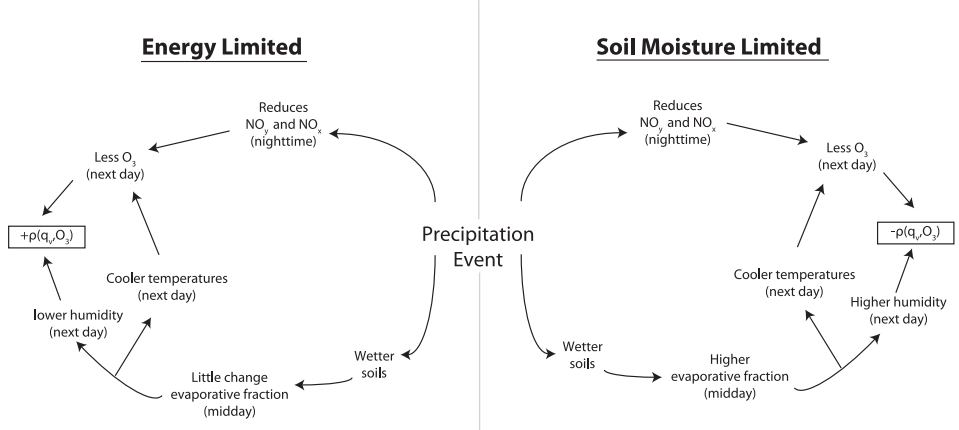

Fig. 7. The proposed chemical and meteorological pathways producing the ozone–humidity correlations under energy-limited (north of 37°N) and soil moisture-limited (south of 37°N) evapotranspiration regimes.

illustrated in the simultaneous sharp decrease in temperature and humidity prior to low ozone events under energy-limited regimes (Fig. 5a and c). Because evapotranspiration is energy-limited, additional soil water provided by the synoptic precipitation has a weak influence on evaporative fraction (Fig. 5d). Further, hours prior to high O_3 days (>70 ppb) show slightly lower evaporative fraction (e.g. drier soil) and higher humidity (Fig. 5c and d) illustrating the weak control surface soil drying has on near-surface humidity. We speculate that the positive correlation between humidity and ozone found over the Northeastern US is likely driven by air mass changes following the passage of mid-latitude synoptic systems producing low ozone production conditions (cooler temperatures, ozone precursor removal, and outflow). This is in agreement with Li et al. (2005) and Leibensperger et al. (2008) who demonstrated the importance of mid-latitude systems for venting pollution episodes north of 35°N and 40°N.

Under soil moisture-limited conditions (south of 37°N), precipitation events are characterized by convective activity. Similar to energy-limited regimes, convective precipitation events effectively remove surface NO_y species (Fig. 6d) reducing subsequent day ozone (Fig. 6a). However, unlike energy-limited regimes, additional soil moisture provided by precipitation increases the evaporative fraction (Fig. 5d) and energy partitioned toward evapotranspiration instead of sensible heat flux. This reduction in sensible heat flux decreases near-surface temperatures (Fig. 5a) and increases evapotranspiration producing higher surface humidity (Fig. 5c). Therefore, the negative correlation between humidity and ozone is likely an artifact of coincident cooler temperatures, removal and ventilation of ozone and ozone precursors, and subsequent increases in evapotranspiration and humidity following precipitation over the Southeast. The transition from the energy-limited Northeast to the soil moisture-limited Southeast may provide an explanation for the north-south change in sign of ozone–humidity correlations (Fig. 1c) and weakening of the ozone–temperature correlation (Fig. 1b).

Because the ozone–humidity correlation is likely a manifestation of soil moisture–atmosphere coupling regimes, evaporative fraction could be a better predictor of ozone over the Southeastern US than temperature or humidity (Fig. 4b). The utility of evaporative fraction as a predictor arises from its ability to retain information of prior precipitation events (e.g. wet removal and ventilation) and instantaneous meteorological conditions (temperature and radiation) relevant to ozone production. Therefore, evaporative fraction could be a useful diagnostic encompassing both chemical and meteorological factors contributing to O_3 formation rather than a direct control variable. The capability of evaporative fraction to be used as a predictor weakens in energy-limited regimes because, as defined by the land–atmosphere coupling framework, the land surface exerts weaker influence over atmospheric states.

Past studies indicate that the NLDAS-MOSAIC model overestimates evapotranspiration and underestimates sensible heat flux relative to other land models and observations during the summer (Robock et al., 2003; Mo et al., 2011; Xia et al., 2012b). This discrepancy in energy partitioning places the transition from soil moisture-to-energy limited regimes farther north than other models (Xia et al., 2012a), however, all four land surface models used by NLDAS2 identified soil water-limited evapotranspiration south of 36°N during the summer over the Eastern US (Xia et al., 2012a). Therefore, analysis of the mechanism over the ATL and NE focus regions (Figs. 5 and 6) are not likely influenced by the choice of NLDAS2-MOSAIC.

5. Concluding remarks

We demonstrate the potential importance of soil moisture and surface energy partitioning in describing a physical mechanism underlying the north-south O_3-meteorology correlations over the Eastern US using 17-years of observed EPA-AQS and NLDAS2 reanalysis data. We show that the distinct north-south gradients of temperature-ozone and humidity-ozone correlations (Camalier et al., 2007; Zheng et al., 2007; Davis et al., 2011; Rasmussen et al., 2012) likely arise from land–atmosphere coupling regimes. Specifically, it is proposed that near-surface humidity is a passive surrogate in ozone formation reflecting the simultaneous impact of surface drying on near-surface humidity and other ozone formation factors (temperature and radiation) in the Southeast. Because it is difficult to identify causal relationships of individual variables within the highly coupled climate–chemistry system, analyzing ozone concentration behavior from the perspective of land–atmosphere coupling provides guidance for understanding the impact of climate on surface ozone. We showed that the evaporative fraction returned a higher correlation with O_3 concentrations than temperature, humidity, or radiation for the Southeastern US due to its ability to capture prior day precipitation and instantaneous environmental variables relevant for O_3 photochemical production. The ozone–evaporative fraction correlation may therefore serve as a simple and useful diagnostic for assessing the degree of climate–chemistry interactions within fully interactive and offline chemistry models. Because the surface flux data needed to calculate the evaporative fraction are not widely available, this work highlights the need for co-located chemical, surface flux, and atmospheric measurements. The land–atmosphere coupling framework may also provide insight into the inability of chemistry–climate models to reproduce observed O_3-temperature relationships (Rasmussen et al., 2012) and the systematic overestimate of modeled ozone (greater than 10 ppb) over the Southeastern US (Fiore et al., 2009; Reidmiller et al., 2009). This work provides motivation for further investigation into the proposed mechanism and utility of the evaporative fraction using climate–chemistry models and other long-term chemical observations.

Acknowledgments

We thank the two anonymous reviewers for their helpful and constructive comments. Portions of this work were supported by the NSF ATM 0809255 and the U.S.-Egypt Joint Science and Technology Fund. NLDAS2 data were acquired as part of the mission of NASA's Earth Science Division and archived and distributed by the Goddard Earth Sciences (GES) Data and Information Services Center (DISC).

Appendix A. Supplementary material

Supplementary material related to this article can be found at http://dx.doi.org/10.1016/j.atmosenv.2013.03.002.

References

Betts, A.K., 2004. Understanding hydrometeorology using global models. Bulletin of the American Meteorological Society 85, 1673. http://dx.doi.org/10.1175/bams-85-11-1673.

Betts, A.K., 2009. Land–surface–atmosphere coupling in observations and models. Journal of Advances in Modeling Earth Systems 1. http://dx.doi.org/10.3894/James.2009.1.4. Artn 4.

Blanchard, C.L., Hidy, G.M., Tanenbaum, S., 2010. Nmoc, ozone, and organic aerosol in the Southeastern United States, 1999–2007 2 ozone trends and sensitivity to Nmoc emissions in Atlanta, Georgia. Atmospheric Environment 44, 4840–4849. http://dx.doi.org/10.1016/j.atmosenv.2010.07.030.

Bloomer, B.J., Stehr, J.W., Piety, C.A., Salawitch, R.J., Dickerson, R.R., 2009. Observed relationships of ozone air pollution with temperature and emissions. Geophysical Research Letters 36. http://dx.doi.org/10.1029/2009gl037308. Artn L09803.

Camalier, L., Cox, W., Dolwick, P., 2007. The effects of meteorology on ozone in urban areas and their use in assessing ozone trends. Atmospheric Environment 41, 7127–7137. http://dx.doi.org/10.1016/j.atmosenv.2007.04.061.

Chameides, W.L., Lindsay, R.W., Richardson, J., Kiang, C.S., 1988. The role of biogenic hydrocarbons in urban photochemical Smog – Atlanta as a case-study. Science 241, 1473–1475.

Cosgrove, B.A., Lohmann, D., Mitchell, K.E., Houser, P.R., Wood, E.F., Schaake, J.C., Robock, A., Sheffield, J., Duan, Q.Y., Luo, L.F., Higgins, R.W., Pinker, R.T., Tarpley, J.D., 2003. Land surface model spin-up behavior in the north American land data assimilation system (Nldas). Journal of Geophysical Research-Atmospheres 108 (19), 8845. http://dx.doi.org/10.1029/2002jd003316.

Cox, W.M., Chu, S.H., 1993. Meteorologically adjusted ozone trends in urban areas – a probabilistic approach. Atmospheric Environment Part B-Urban Atmosphere 27, 425–434.

Daly, C., Neilson, R.P., Phillips, D.L., 1994. A statistical topographic model for mapping climatological precipitation over Mountainous Terrain. Journal of Applied Meteorology 33, 140–158.

Davis, J., Cox, W., Reff, A., Dolwick, P., 2011. A comparison of Cmaq-based and observation-based statistical models relating ozone to meteorological parameters. Atmospheric Environment 45, 3481–3487. http://dx.doi.org/10.1016/J.Atmosenv.2010.12.060.

Dawson, J.P., Adams, P.J., Pandis, S.N., 2007. Sensitivity of ozone to summertime climate in the Eastern USA: a modeling case study. Atmospheric Environment 41, 1494–1511. http://dx.doi.org/10.1016/J.Atmosenv.2006.10.033.

Dirmeyer, P.A., 2011. The terrestrial segment of soil moisture–climate coupling. Geophysical Research Letters 38. http://dx.doi.org/10.1029/2011gl048268. Artn L16702.

Dunlea, E.J., Herndon, S.C., Nelson, D.D., Volkamer, R.M., San Martini, F., Sheehy, P.M., Zahniser, M.S., Shorter, J.H., Wormhoudt, J.C., Lamb, B.K., Allwine, E.J., Gaffney, J.S., Marley, N.A., Grutter, M., Marquez, C., Blanco, S., Cardenas, B., Retama, A., Villegas, C.R.R., Kolb, C.E., Molina, L.T., Molina, M.J., 2007. Evaluation of nitrogen dioxide chemiluminescence monitors in a polluted urban environment. Atmospheric Chemistry and Physics 7, 2691–2704.

Fang, Y.Y., Fiore, A.M., Horowitz, L.W., Gnanadesikan, A., Levy, H., Hu, Y.T., Russell, A.G., 2009. Estimating the contribution of strong daily export events to total pollutant export from the United States in summer. Journal of Geophysical Research-Atmospheres 114. http://dx.doi.org/10.1029/2008jd010946. Artn D23302.

Fehsenfeld, F.C., Dickerson, R.R., Hubler, G., Luke, W.T., Nunnermacker, L.J., Williams, E.J., Roberts, J.M., Calvert, J.G., Curran, C.M., Delany, A.C., Eubank, C.S., Fahey, D.W., Fried, A., Gandrud, B.W., Langford, A.O., Murphy, P.C., Norton, R.B., Pickering, K.E., Ridley, B.A., 1987. A ground-based intercomparison of No, Nox, and Noy measurement techniques. Journal of Geophysical Research-Atmospheres 92, 14710–14722. http://dx.doi.org/10.1029/Jd092id12p14710.

Fennessy, M.J., Shukla, J., 1999. Impact of initial soil wetness on seasonal atmospheric prediction. Journal of Climate 12, 3167–3180.

Findell, K.L., Eltahir, E.A.B., 1997. An analysis of the soil moisture-rainfall feedback, based on direct observations from Illinois. Water Resources Research 33, 725–735.

Fiore, A.M., Dentener, F.J., Wild, O., Cuvelier, C., Schultz, M.G., Hess, P., Textor, C., Schulz, M., Doherty, R.M., Horowitz, L.W., MacKenzie, I.A., Sanderson, M.G., Shindell, D.T., Stevenson, D.S., Szopa, S., Van Dingenen, R., Zeng, G., Atherton, C., Bergmann, D., Bey, I., Carmichael, G., Collins, W.J., Duncan, B.N., Faluvegi, G., Folberth, G., Gauss, M., Gong, S., Hauglustaine, D., Holloway, T., Isaksen, I.S.A., Jacob, D.J., Jonson, J.E., Kaminski, J.W., Keating, T.J., Lupu, A., Marmer, E., Montanaro, V., Park, R.J., Pitari, G., Pringle, K.J., Pyle, J.A., Schroeder, S., Vivanco, M.G., Wind, P., Wojcik, G., Wu, S., Zuber, A., 2009. Multimodel estimates of intercontinental source-receptor relationships for ozone pollution. Journal of Geophysical Research-Atmospheres 114. http://dx.doi.org/10.1029/2008jd010816. Artn D04301.

Fiore, A.M., Horowitz, L.W., Purves, D.W., Levy, H., Evans, M.J., Wang, Y.X., Li, Q.B., Yantosca, R.M., 2005. Evaluating the contribution of changes in isoprene emissions to surface ozone trends over the Eastern United States. Journal of Geophysical Research-Atmospheres 110. http://dx.doi.org/10.1029/2004jd005485.

Fischer, E.M., Seneviratne, S.I., Luthi, D., Schar, C., 2007. Contribution of land–atmosphere coupling to recent European summer heat waves. Geophysical Research Letters 34. http://dx.doi.org/10.1029/2006gl029068.

Frost, G.J., McKeen, S.A., Trainer, M., Ryerson, T.B., Neuman, J.A., Roberts, J.M., Swanson, A., Holloway, J.S., Sueper, D.T., Fortin, T., Parrish, D.D., Fehsenfeld, F.C., Flocke, F., Peckham, S.E., Grell, G.A., Kowal, D., Cartwright, J., Auerbach, N., Habermann, T., 2006. Effects of changing power plant No(X) emissions on ozone in the Eastern United States: proof of concept. Journal of Geophysical Research-Atmospheres 111. http://dx.doi.org/10.1029/2005jd006354. Artn D12306.

Guenther, A., Karl, T., Harley, P., Wiedinmyer, C., Palmer, P.I., Geron, C., 2006. Estimates of global terrestrial isoprene emissions using Megan (model of emissions of gases and aerosols from nature). Atmospheric Chemistry and Physics 6, 3181–3210.

Guenther, A., Zimmerman, P., Wildermuth, M., 1994. Natural volatile organic-compound emission rate estimates for United-States Woodland Landscapes. Atmospheric Environment 28, 1197–1210.

Guo, Z.C., Dirmeyer, P.A., DelSole, T., 2011. Land surface impacts on subseasonal and seasonal predictability. Geophysical Research Letters 38. http://dx.doi.org/10.1029/2011gl049945. Artn L24812.

Higgins, R.W., Janowiak, J., Yao, Y., 1996. A Gridded Hourly Precipitation Data Base for the United States (1963–1993). NCEP/Climate Prediction Center ATLAS. p. 47.

Jacobson, M.Z., 1999. Effects of soil moisture on temperatures, winds, and pollutant concentrations in Los Angeles. Journal of Applied Meteorology 38, 607–616.

Johnson, C.E., Collins, W.J., Stevenson, D.S., Derwent, R.G., 1999. Relative roles of climate and emissions changes on future tropospheric oxidant concentrations. Journal of Geophysical Research-Atmospheres 104, 18631–18645.

Kleinman, L.I., Daum, P.H., Lee, Y.N., Nunnermacker, L.J., Springston, S.R., Weinstein-Lloyd, J., Rudolph, J., 2005. A comparative study of ozone production in five U.S. Metropolitan areas. Journal of Geophysical Research-Atmospheres 110. http://dx.doi.org/10.1029/2004jd005096.

Koster, R.D., Guo, Z.C., Dirmeyer, P.A., Bonan, G., Chan, E., Cox, P., Davies, H., Gordon, C.T., Kanae, S., Kowalczyk, E., Lawrence, D., Liu, P., Lu, C.H., Malyshev, S., McAvaney, B., Mitchell, K., Mocko, D., Oki, T., Oleson, K.W., Pitman, A., Sud, Y.C., Taylor, C.M., Verseghy, D., Vasic, R., Xue, Y.K., Yamada, T., 2006. Glace: the global land–atmosphere coupling experiment. Part I: Overview. Journal of Hydrometeorology 7, 590–610.

Koster, R.D., Mahanama, S.P.P., Yamada, T.J., Balsamo, G., Berg, A.A., Boisserie, M., Dirmeyer, P.A., Doblas-Reyes, F.J., Drewitt, G., Gordon, C.T., Guo, Z., Jeong, J.H., Lawrence, D.M., Lee, W.S., Li, Z., Luo, L., Malyshev, S., Merryfield, W.J., Seneviratne, S.I., Stanelle, T., van den Hurk, B., Vitart, F., Wood, E.F., 2010. Contribution of land surface initialization to subseasonal forecast skill: first results from a multi-model experiment. Geophysical Research Letters 37, 6. http://dx.doi.org/10.1029/2009gl041677. L02402.

Koster, R.D., Schubert, S.D., Suarez, M.J., 2009. Analyzing the concurrence of meteorological droughts and warm periods, with implications for the determination of evaporative regime. Journal of Climate 22, 3331–3341. http://dx.doi.org/10.1175/2008jcli2718.1.

Koster, R.D., Suarez, M.J., 1992. Modeling the land surface boundary in climate models as a composite of independent vegetation stands. Journal of Geophysical Research-Atmospheres 97, 2697–2715.

Koster, R.D., Suarez, M.J., 1994. The components of a Svat scheme and their effects on a Gcms hydrological cycle. Advances in Water Resources 17, 61–78.

Leibensperger, E.M., Mickley, L.J., Jacob, D.J., 2008. Sensitivity of US air quality to mid-latitude cyclone frequency and implications of 1980–2006 climate change. Atmospheric Chemistry and Physics 8, 7075–7086.

Li, Q.B., Jacob, D.J., Park, R., Wang, Y.X., Heald, C.L., Hudman, R., Yantosca, R.M., Martin, R.V., Evans, M., 2005. North American pollution outflow and the trapping of convectively lifted pollution by upper-level anticyclone. Journal of Geophysical Research-Atmospheres 110. http://dx.doi.org/10.1029/2004jd005039. Artn D10301.

Luo, L.F., Wood, E.F., 2007. Monitoring and predicting the 2007 U.S. Drought. Geophysical Research Letters 34, L22702. http://dx.doi.org/10.1029/2007GL031673.

Merrill, J.T., Moody, J.L., 1996. Synoptic meteorology and transport during the North Atlantic Regional experiment (Nare) intensive: overview. Journal of Geophysical Research-Atmospheres 101, 28903–28921. http://dx.doi.org/10.1029/96jd00097.

Mesinger, F., DiMego, G., Kalnay, E., Mitchell, K., Shafran, P.C., Ebisuzaki, W., Jovic, D., Woollen, J., Rogers, E., Berbery, E.H., Ek, M.B., Fan, Y., Grumbine, R., Higgins, W., Li, H., Lin, Y., Manikin, G., Parrish, D., Shi, W., 2006. North American regional reanalysis. Bulletin of the American Meteorological Society 87, 343. http://dx.doi.org/10.1175/Bams-87-3-343.

Miralles, D.G., van den Berg, M.J., Teuling, A.J., de Jeu, R.A.M., 2012. Soil moisture–temperature coupling: a multiscale observational analysis. Geophysical Research Letters 39, L21707. http://dx.doi.org/10.1029/2012GL053703.

Mitchell, K.E., Lohmann, D., Houser, P.R., Wood, E.F., Schaake, J.C., Robock, A., Cosgrove, B.A., Sheffield, J., Duan, Q.Y., Luo, L.F., Higgins, R.W., Pinker, R.T., Tarpley, J.D., Lettenmaier, D.P., Marshall, C.H., Entin, J.K., Pan, M., Shi, W., Koren, V., Meng, J., Ramsay, B.H., Bailey, A.A., 2004. The multi-institution North American land data Assimilation system (Nldas): utilizing multiple Gcip products and partners in a continental distributed hydrological modeling system. Journal of Geophysical Research-Atmospheres 109, 32. http://dx.doi.org/10.1029/2003jd003823. D07s90.

Mo, K.C., Long, L.N., Xia, Y.L., Yang, S.K., Schemm, J.E., Ek, M., 2011. Drought indices based on the climate forecast system reanalysis and ensemble Nldas. Journal of Hydrometeorology 12, 181–205. http://dx.doi.org/10.1175/2010jhm1310.1.

Pal, J.S., Eltahir, E.A.B., 2001. Pathways relating soil moisture conditions to future summer rainfall within a model of the land–atmosphere system. Journal of Climate 14, 1227–1242.

Petron, G., Harley, P., Greenberg, J., Guenther, A., 2001. Seasonal temperature variations influence isoprene emission. Geophysical Research Letters 28, 1707–1710.

Pickering, K.E., Dickerson, R.R., Huffman, G.J., Boatman, J.F., Schanot, A., 1988. Trace Gas-Transport in the vicinity of frontal convective clouds. Journal of Geophysical Research-Atmospheres 93, 759–773. http://dx.doi.org/10.1029/JD093iD01p00759.

Pinker, R.T., Tarpley, J.D., Laszlo, I., Mitchell, K.E., Houser, P.R., Wood, E.F., Schaake, J.C., Robock, A., Lohmann, D., Cosgrove, B.A., Sheffield, J., Duan, Q.Y., Luo, L.F., Higgins, R.W., 2003. Surface radiation budgets in support of the Gewex continental-scale international project (Gcip) and the Gewex Americas prediction Project (Gapp), including the North American Land Data Assimilation system (Nldas) Project. Journal of Geophysical Research-Atmospheres 108. http://dx.doi.org/10.1029/2002jd003301. Artn 8844.

Rasmussen, D.J., Fiore, A.M., Naik, V., Horowitz, L.W., McGinnis, S.J., Schultz, M.G., 2012. Surface ozone-temperature relationships in the Eastern US: a monthly climatology for evaluating chemistry-climate models. Atmospheric Environment 47, 142–153. http://dx.doi.org/10.1016/j.atmosenv.2011.11.021.

Reidmiller, D.R., Fiore, A.M., Jaffe, D.A., Bergmann, D., Cuvelier, C., Dentener, F.J., Duncan, B.N., Folberth, G., Gauss, M., Gong, S., Hess, P., Jonson, J.E., Keating, T.,

Lupu, A., Marmer, E., Park, R., Schultz, M.G., Shindell, D.T., Szopa, S., Vivanco, M.G., Wild, O., Zuber, A., 2009. The influence of Foreign Vs. North American emissions on surface ozone in the US. Atmospheric Chemistry and Physics 9, 5027–5042.

Robock, A., Luo, L.F., Wood, E.F., Wen, F.H., Mitchell, K.E., Houser, P.R., Schaake, J.C., Lohmann, D., Cosgrove, B., Sheffield, J., Duan, Q.Y., Higgins, R.W., Pinker, R.T., Tarpley, J.D., Basara, J.B., Crawford, K.C., 2003. Evaluation of the North American Land Data Assimilation system over the Southern Great Plains during the warm season. Journal of Geophysical Research-Atmospheres 108. http://dx.doi.org/10.1029/2002jd003245. Artn 8846.

Santanello, J.A., Peters-Lidard, C.D., Kumar, S.V., 2011. Diagnosing the sensitivity of local land–atmosphere coupling via the soil moisture-boundary layer interaction. Journal of Hydrometeorology 12, 766–786. http://dx.doi.org/10.1175/JhmD-10-05014.1.

Seneviratne, S.I., Corti, T., Davin, E.L., Hirschi, M., Jaeger, E.B., Lehner, I., Orlowsky, B., Teuling, A.J., 2010. Investigating soil moisture–climate interactions in a changing climate: a review. Earth-Science Reviews 99, 125–161. http://dx.doi.org/10.1016/J.Earscirev.2010.02.004.

Seneviratne, S.I., Luthi, D., Litschi, M., Schar, C., 2006. Land–atmosphere coupling and climate change in Europe. Nature 443, 205–209. http://dx.doi.org/10.1038/nature05095.

Sickles, J.E., Shadwick, D.S., 2007. Seasonal and regional air quality and atmospheric deposition in the Eastern United States. Journal of Geophysical Research-Atmospheres 112. http://dx.doi.org/10.1029/2006jd008356. Artn D17302.

Sillman, S., Samson, F.J., 1995. Impact of temperature on oxidant photochemistry in urban, polluted rural and remote environments. Journal of Geophysical Research-Atmospheres 100, 11497–11508.

Steiner, A.L., Davis, A.J., Sillman, S., Owen, R.C., Michalak, A.M., Fiore, A.M., 2010. Observed suppression of ozone formation at extremely high temperatures due to chemical and biophysical feedbacks. Proceedings of National Academy of Sciences of the United States of America 107, 19685–19690. http://dx.doi.org/10.1073/pnas.1008336107.

Steiner, A.L., Tonse, S., Cohen, R.C., Goldstein, A.H., Harley, R.A., 2006. Influence of future climate and emissions on Regional air quality in California. Journal of Geophysical Research-Atmospheres 111. http://dx.doi.org/10.1029/2005jd006935. Artn D18303.

Vukovich, F.M., 1995. Regional-scale boundary-layer ozone variations in the Eastern United-States and their association with meteorological variations. Atmospheric Environment 29, 2259–2273.

Whelpdale, D.M., Low, T.B., Kolomeychuk, R.J., 1984. Advection climatology for the East Coast of North-America. Atmospheric Environment 18, 1311–1327. http://dx.doi.org/10.1016/0004-6981(84)90040-4.

Wu, W.R., Dickinson, R.E., Wang, H., Liu, Y.Q., Shaikh, M., 2007. Covariabilities of Spring soil moisture and summertime United States precipitation in a climate simulation. International Journal of Climatology 27, 429–438. http://dx.doi.org/10.1002/joc.1419.

Xia, Y.L., Ek, M., Wei, H.L., Meng, J., 2012a. Comparative analysis of relationships between Nldas-2 forcings and model outputs. Hydrological Processes 26, 467–474. http://dx.doi.org/10.1002/Hyp.8240.

Xia, Y.L., Mitchell, K., Ek, M., Sheffield, J., Cosgrove, B., Wood, E., Luo, L.F., Alonge, C., Wei, H.L., Meng, J., Livneh, B., Lettenmaier, D., Koren, V., Duan, Q.Y., Mo, K., Fan, Y., Mocko, D., 2012b. Continental-scale water and energy flux analysis and validation for the North American land data Assimilation System Project Phase 2(Nldas-2): 1. Intercomparison and application of model products. Journal of Geophysical Research-Atmospheres 117. http://dx.doi.org/10.1029/2011jd016048. Artn D03109.

Xie, P.P., Arkin, P.A., 1997. Global precipitation: a 17-Year monthly analysis based on gauge observations, satellite estimates, and numerical model outputs. Bulletin of the American Meteorological Society 78, 2539–2558.

Zeng, G., Pyle, J.A., Young, P.J., 2008. Impact of climate change on tropospheric ozone and its global budgets. Atmospheric Chemistry and Physics 8, 369–387.

Zheng, J., Swall, J.L., Cox, W.M., Davis, J.M., 2007. Interannual variation in meteorologically adjusted ozone levels in the Eastern United States: a comparison of two approaches. Atmospheric Environment 41, 705–716. http://dx.doi.org/10.1016/J.Atmosenv.2006.09.010.